

JAERI-Research

96-061



JT-60U THOMSON SCATTERING SYSTEM  
WITH MULTIPLE RUBY LASERS AND HIGH SPATIAL RESOLUTION  
FOR HIGH ELECTRON TEMPERATURE PLASMA MEASUREMENT

November 1996

Hidetoshi YOSHIDA, Osamu NAITO, Osamu YAMASHITA,  
Shigeru KITAMURA Takaki HATAE and Akira NAGASHIMA

日本原子力研究所  
Japan Atomic Energy Research Institute

本レポートは、日本原子力研究所が不定期に公刊している研究報告書です。

入手の問合わせは、日本原子力研究所研究情報部研究情報課（〒319-11 茨城県那珂郡東海村）あて、お申し越してください。なお、このほかに財団法人原子力弘済会資料センター（〒319-11 茨城県那珂郡東海村日本原子力研究所内）で複写による実費頒布をおこなっております。

This report is issued irregularly.

Inquiries about availability of the reports should be addressed to Research Information Division, Department of Intellectual Resources, Japan Atomic Energy Research Institute, Tokai-mura, Naka-gun, Ibaraki-ken, 319-11, Japan.

© Japan Atomic Energy Research Institute, 1996

編集兼発行 日本原子力研究所  
印 刷 いばらき印刷(株)

JT-60U Thomson Scattering System with Multiple Ruby Laser and High Spatial Resolution  
for High Electron Temperature Plasma Measurement

Hidetoshi YOSHIDA, Osamu NAITO, Osamu YAMASHITA, Shigeru KITAMURA  
Takaki HATAE and Akira NAGASHIMA

Department of Fusion Plasma Research  
Naka Fusion Research Establishment  
Japan Atomic Energy Research Institute  
Naka-machi, Naka-gun, Ibaraki-ken

(Received October 22, 1996)

This article describes the design and operation of a 60 spatial channel Thomson scattering system as of 1996 with multiple ruby lasers to measure the electron temperature  $T_e$  and density  $n_e$  profiles of the JT-60U plasmas. The wide spectral range (403~683 nm) of the spectrometer and newly developed two-dimensional detector (high repetition photodiode array) has enabled this system to measure the high electron temperature plasma (5 keV or more) formed at the plasma core during negative magnetic shear discharge with high precision and reliability. The high spatial resolution (8 mm) have provided the precise measurement of steep electron temperature and density gradients formed at the plasma edge and in the scrape-off layer during H-mode discharge. The multilaser operation with the minimum time interval of 2 ms has provided an essential tool for the transient phenomenon measurement like the formation process of edge transport barrier during L- to H-mode transition and internal transport barrier during discharge with negative magnetic shear, the relaxation process of pellet injected plasma and so on. Measurement examples of recent JT-60U  $T_e$  and  $n_e$  profiles are also presented.

Keywords: JT-60U, Thomson Scattering, Multilaser, Electron Temperature, Electron Density, Photodiode Array, H-mode, Negative Shear, Pellet Injection, Transport Barrier

高温プラズマ測定のためのJT-60U用高空間分解マルチレーザー  
トムソン散乱計測システム

日本原子力研究所那珂研究所炉心プラズマ研究部  
吉田 英俊・内藤 磨・山下 修・北村 繁  
波多江仰紀・長島 章

(1996年10月22日受理)

本論文は、高温なJT-60Uプラズマの電子温度  $T_e$  と電子密度  $n_e$  をマルチレーザーを活用して空間点数60点で測定するトムソン散乱計測システムについて、その1996年現在までの設計及び測定実績を記述する。分光器と新開発の2次元検出器（高速計測可能型フォトダイオードアレイ）の高スペクトル帯域化（波長403～683nmまでカバー）によって、高精度かつ高い信頼性を確保しつつ負磁気シア放電で炉心内部に形成される高電子温度プラズマの測定を可能にした。また高空間分解能（8mm）測定によって、Hモード放電でプラズマ周辺部及びスクレイブオフ層に形成される  $T_e$  と  $n_e$  の急峻な勾配の正確な測定を可能にした。最小時間差2ミリ秒のマルチレーザーの活用は、LモードからHモードへの遷移に伴う周辺輸送障壁や負磁気シア放電での内部輸送障壁の形成過程、また固体燃料ペレットを入射した後のプラズマの緩和過程、等々の過渡現象測定に必要不可欠なものとなった。本論文では、JT-60Uプラズマの  $T_e$  と  $n_e$  分布の最近の測定例についても言及する。

Contents

1. Introduction .....	1
2. Multiple Ruby Laser System .....	1
3. Collection Optics, Fiber Optics and Alignment System .....	2
4. Spectrometers and PDA/PMT Detector Systems .....	2
5. Data Acquisition System and Data Processing System .....	3
6. Measurement Examples and Related Discussions .....	3
7. Conclusion .....	4
Acknowledgments .....	6
References .....	7

目 次

1. 序 論 .....	1
2. マルチルビーレーザーシステム .....	1
3. 集光光学系、ファイバー光学系及びアライメントシステム .....	2
4. 分光器及びPDA/PMT検出器システム .....	2
5. データ収集系及びデータ処理系 .....	3
6. 測定例及び議論 .....	3
7. 結 論 .....	4
謝 辞 .....	6
参考文献 .....	7

## 1. Introduction

Thomson scattering system is an only plasma diagnostic that can measure precisely and absolutely the electron temperature  $T_e$  and density  $n_e$  profile at one time. It has been used as an essential diagnostic tool widely in tokamak plasma experiments for about 30 years. So far a number of different approaches have been developed for aiming at more spatial points and higher repetition.<sup>1)-7)</sup> As the plasma performance has been improved better with its larger device size, the reliability for higher  $T_e$  plasma measurement has been also an key issue to be considered.

In order to fit the JT-60 Upgrade configuration and its experimental purposes, a new Thomson scattering system for the JT-60U has been constructed concentratively at the period of 1990 to 1991 and continuously for a few years. The old Thomson scattering<sup>6)</sup> was partially rebuilt and improved in the new system. Since 1991 the JT-60U Thomson scattering system has been gradually in operation. This system is characterized by the high-spatially-resolved multipoint measurement of 60 channels with the flexibility concerning the multi-ruby-laser operation. The main purpose of this paper is to describe the overview on its design concept in Section 2~5, to introduce especially a novel two-dimensional detector with high repetition suited for higher  $T_e$  measurement in Section 4, and to present recent examples of the  $T_e$  and  $n_e$  profile measurements in Section 6 together with related discussions. The conclusion in this work is summarized in Section 7.

## 2. Multiple Ruby Laser System

The system layout for the present ruby Thomson as of 1995 is shown in Fig. 1. Using a beam combiner composed of a polarizer plate and a Faraday rotator, two ruby lasers with 10 J, 30 ns of pulse width and a single beam path line have provided the transient phenomena measurement such as L- to H-mode transition and pellet injection with the minimum time difference of 2ms in the burst mode operation, or of the multi-time-slice measurement with the repetition rate of ~0.5 Hz in the normal mode operation.<sup>8)</sup> The detailed parameters of the two lasers and the beam combiner are summarized in Table I. For the reliable electron density measurement with the multilaser Thomson scattering, the relative beam energy of the two ruby lasers is stably and precisely monitored by a PIN diode in the laser room through a communication optical fiber ~300 m long which guides the laser light uniformly averaged by an integrating sphere located at the beam dump.

## 1. Introduction

Thomson scattering system is an only plasma diagnostic that can measure precisely and absolutely the electron temperature  $T_e$  and density  $n_e$  profile at one time. It has been used as an essential diagnostic tool widely in tokamak plasma experiments for about 30 years. So far a number of different approaches have been developed for aiming at more spatial points and higher repetition.<sup>1)-7)</sup> As the plasma performance has been improved better with its larger device size, the reliability for higher  $T_e$  plasma measurement has been also an key issue to be considered.

In order to fit the JT-60 Upgrade configuration and its experimental purposes, a new Thomson scattering system for the JT-60U has been constructed concentratively at the period of 1990 to 1991 and continuously for a few years. The old Thomson scattering<sup>6)</sup> was partially rebuilt and improved in the new system. Since 1991 the JT-60U Thomson scattering system has been gradually in operation. This system is characterized by the high-spatially-resolved multipoint measurement of 60 channels with the flexibility concerning the multi-ruby-laser operation. The main purpose of this paper is to describe the overview on its design concept in Section 2~5, to introduce especially a novel two-dimensional detector with high repetition suited for higher  $T_e$  measurement in Section 4, and to present recent examples of the  $T_e$  and  $n_e$  profile measurements in Section 6 together with related discussions. The conclusion in this work is summarized in Section 7.

## 2. Multiple Ruby Laser System

The system layout for the present ruby Thomson as of 1995 is shown in Fig. 1. Using a beam combiner composed of a polarizer plate and a Faraday rotator, two ruby lasers with 10 J, 30 ns of pulse width and a single beam path line have provided the transient phenomena measurement such as L- to H-mode transition and pellet injection with the minimum time difference of 2ms in the burst mode operation, or of the multi-time-slice measurement with the repetition rate of ~0.5 Hz in the normal mode operation.<sup>8)</sup> The detailed parameters of the two lasers and the beam combiner are summarized in Table I. For the reliable electron density measurement with the multilaser Thomson scattering, the relative beam energy of the two ruby lasers is stably and precisely monitored by a PIN diode in the laser room through a communication optical fiber ~300 m long which guides the laser light uniformly averaged by an integrating sphere located at the beam dump.

### 3. Collection Optics, Fiber Optics and Alignment System

As shown in Fig. 2, two kinds of collection optics have been working: Cassegrain type mirrors located at the *RI* port viewing the core plasma with the spatial resolution of 22 mm (30 spatial points) and double Gaussian lens at the *INIA* port seeing the edge plasma with the spatial resolution of 8 mm (20 spatial points) and 16 mm (10 spatial points). The collected lights are led into three sets of Littrow type grating spectrometer by quartz fiber bundles ~100 m long with about 50% transmission at 632.8 nm. The major parameters of the collection and fiber optics are shown in Table II.

For the accurate  $n_e$  measurement, the direct and quantitative alignment system has been successfully working for monitoring and adjusting the alignment between the object field of the collection fiber optics and the laser beam.<sup>9)</sup> The important and distinctive feature of this new alignment system is to attain the compatibility between a stable and accurate maintenance of alignment and an improvement of the *S/N* ratio of Thomson scattering to plasma light with accompanying the reduced fiber cost. Namely the width of the above quartz fiber bundles could be designed as narrow as the corresponding beam width especially in the *INIA* collection optic, aiming at the reduction of unnecessary plasma light.

### 4. Spectrometers and PDA/PMT Detector Systems

The spectral range of Littrow type grating spectrometer is about 403 nm to 683 nm for the high  $T_e$  plasma core measurement, and 550 nm to 688 nm for the low  $T_e$  plasma edge measurement. The spatially and spectrally resolved output images of the three spectrometers are severally converted to electrical signals by a newly developed high repetition (1 ms) photodiode array (PDA) with spatial and spectral division of 20x12 pixels and also 10x6 PMTs for the core plasma measurement (core PMT), and 30x(4~5) PMTs for the edge plasma measurement (edge PMT). The schematic illustration of the optical and detector systems are given in Fig. 3. The parameters of the spectrometers and coupling optics is listed in Table III, and those of the detector systems in Table IV.

The detector systems consists of the newly developed two-dimensional detector and the conventional PMTs. A photograph of the two-dimensional detector is shown in Fig. 4, which is mainly composed of an image intensifier of proximity focused type (MCP, microchannel plate) and a 240 ch photodiode array with charge sensitive amplifiers as schematically illustrated in Figs. 1 and 5. The spectral division of the PDA was designed to show a full performance in higher  $T_e$  regime of 5~20 keV with 12 spectral pixels for each spatial point as indicated in Fig. 6. Figure 7 shows the data flow of the PDA system. The effective use of parallel data



### 3. Collection Optics, Fiber Optics and Alignment System

As shown in Fig. 2, two kinds of collection optics have been working: Cassegrain type mirrors located at the *RI* port viewing the core plasma with the spatial resolution of 22 mm (30 spatial points) and double Gaussian lens at the *INIA* port seeing the edge plasma with the spatial resolution of 8 mm (20 spatial points) and 16 mm (10 spatial points). The collected lights are led into three sets of Littrow type grating spectrometer by quartz fiber bundles ~100 m long with about 50% transmission at 632.8 nm. The major parameters of the collection and fiber optics are shown in Table II.

For the accurate  $n_e$  measurement, the direct and quantitative alignment system has been successfully working for monitoring and adjusting the alignment between the object field of the collection fiber optics and the laser beam.<sup>9)</sup> The important and distinctive feature of this new alignment system is to attain the compatibility between a stable and accurate maintenance of alignment and an improvement of the *S/N* ratio of Thomson scattering to plasma light with accompanying the reduced fiber cost. Namely the width of the above quartz fiber bundles could be designed as narrow as the corresponding beam width especially in the *INIA* collection optic, aiming at the reduction of unnecessary plasma light.

### 4. Spectrometers and PDA/PMT Detector Systems

The spectral range of Littrow type grating spectrometer is about 403 nm to 683 nm for the high  $T_e$  plasma core measurement, and 550 nm to 688 nm for the low  $T_e$  plasma edge measurement. The spatially and spectrally resolved output images of the three spectrometers are severally converted to electrical signals by a newly developed high repetition (1 ms) photodiode array (PDA) with spatial and spectral division of 20x12 pixels and also 10x6 PMTs for the core plasma measurement (core PMT), and 30x(4~5) PMTs for the edge plasma measurement (edge PMT). The schematic illustration of the optical and detector systems are given in Fig. 3. The parameters of the spectrometers and coupling optics is listed in Table III, and those of the detector systems in Table IV.

The detector systems consists of the newly developed two-dimensional detector and the conventional PMTs. A photograph of the two-dimensional detector is shown in Fig. 4, which is mainly composed of an image intensifier of proximity focused type (MCP, microchannel plate) and a 240 ch photodiode array with charge sensitive amplifiers as schematically illustrated in Figs. 1 and 5. The spectral division of the PDA was designed to show a full performance in higher  $T_e$  regime of 5~20 keV with 12 spectral pixels for each spatial point as indicated in Fig. 6. Figure 7 shows the data flow of the PDA system. The effective use of parallel data

processing can quicken the encoding, digitizing and decoding time up to less than 1 ms, and provide the high repetition response.

On the other hand, the spectral division of the core PMT system to ensure  $T_e$  measurement of 0.1~10 keV with good precision even in lower  $n_e$  regime of less than  $1 \times 10^{19} \text{ m}^{-3}$ . That of the edge PMT system can give a good estimation even for the extremely low  $n_e$  ( $\sim 1 \times 10^{18} \text{ m}^{-3}$ ) and low  $T_e$  ( $\sim 10 \text{ eV}$ ) condition. Since 1991 the edge PMT has been operational, PDA since 1992 and the core PMT since 1993. The two independent groups of the ADC and memory CAMAC have been used for the acquisition of plasma background (BG) light and Thomson scattering (SG) light separately in the PMT signal flow. Shorter time delay in acquiring SG and BG data can reduce more the fluctuation of signal level caused by the edge localized mode (ELM) activity in the subtraction procedure of BG data from SG data. The precise edge profiles of  $T_e$  and  $n_e$  have been possible to be obtained even with giant ELM activity, when the time delay of the SG and BG timings is shortened to less than 200 ns.

## 5. Data Acquisition System and Data Processing System

The Thomson scattering spectrum is reconstructed with the acquired data from the corresponding CAMAC memories and also with the corresponding calibration data of relative sensitivity of spectral channels, spectral slit functions, relative detector and/or amplifier gains, Rayleigh scattered light intensities, laser energy and so on. The estimation of  $T_e$  and  $n_e$  together with their error bars is made through a non-linear least squares fit of fully relativistic Thomson scattering spectrum to measured one. In this procedure a detector shot noise, a plasma background light level and a circuit noise are taken into consideration. As the fully relativistic Thomson scattering spectrum, an analytic formula is used which is applicable to a wide range of plasmas with extremely high accuracy of less than 0.1% at 100 keV.<sup>10)</sup>

## 6. Measurement Examples and Related Discussions

The multilaser operation has been utilized in the transient phenomena measurements of L- to H-mode transition experiments, negative magnetic shear experiments, the pellet injection experiments and so on. Figure 8 shows the  $T_e$  and  $n_e$  profiles just before and 10 ms after the pellet injection to the OH plasma. The particle fueling in the center region of plasma volume by the pellet injection is clearly observed from the change of  $n_e$  profiles before and after the pellet injection.

The precise profiles of  $T_e$  and  $n_e$ , which were obtained through the plasma edge measurement system including the collection and fiber optics with the high spatial resolution (8 mm), the

processing can quicken the encoding, digitizing and decoding time up to less than 1 ms, and provide the high repetition response.

On the other hand, the spectral division of the core PMT system to ensure  $T_e$  measurement of 0.1~10 keV with good precision even in lower  $n_e$  regime of less than  $1 \times 10^{19} \text{ m}^{-3}$ . That of the edge PMT system can give a good estimation even for the extremely low  $n_e$  ( $\sim 1 \times 10^{18} \text{ m}^{-3}$ ) and low  $T_e$  ( $\sim 10 \text{ eV}$ ) condition. Since 1991 the edge PMT has been operational, PDA since 1992 and the core PMT since 1993. The two independent groups of the ADC and memory CAMAC have been used for the acquisition of plasma background (BG) light and Thomson scattering (SG) light separately in the PMT signal flow. Shorter time delay in acquiring SG and BG data can reduce more the fluctuation of signal level caused by the edge localized mode (ELM) activity in the subtraction procedure of BG data from SG data. The precise edge profiles of  $T_e$  and  $n_e$  have been possible to be obtained even with giant ELM activity, when the time delay of the SG and BG timings is shortened to less than 200 ns.

## 5. Data Acquisition System and Data Processing System

The Thomson scattering spectrum is reconstructed with the acquired data from the corresponding CAMAC memories and also with the corresponding calibration data of relative sensitivity of spectral channels, spectral slit functions, relative detector and/or amplifier gains, Rayleigh scattered light intensities, laser energy and so on. The estimation of  $T_e$  and  $n_e$  together with their error bars is made through a non-linear least squares fit of fully relativistic Thomson scattering spectrum to measured one. In this procedure a detector shot noise, a plasma background light level and a circuit noise are taken into consideration. As the fully relativistic Thomson scattering spectrum, an analytic formula is used which is applicable to a wide range of plasmas with extremely high accuracy of less than 0.1% at 100 keV.<sup>10)</sup>

## 6. Measurement Examples and Related Discussions

The multilaser operation has been utilized in the transient phenomena measurements of L- to H-mode transition experiments, negative magnetic shear experiments, the pellet injection experiments and so on. Figure 8 shows the  $T_e$  and  $n_e$  profiles just before and 10 ms after the pellet injection to the OH plasma. The particle fueling in the center region of plasma volume by the pellet injection is clearly observed from the change of  $n_e$  profiles before and after the pellet injection.

The precise profiles of  $T_e$  and  $n_e$ , which were obtained through the plasma edge measurement system including the collection and fiber optics with the high spatial resolution (8 mm), the

processing can quicken the encoding, digitizing and decoding time up to less than 1 ms, and provide the high repetition response.

On the other hand, the spectral division of the core PMT system to ensure  $T_e$  measurement of 0.1~10 keV with good precision even in lower  $n_e$  regime of less than  $1 \times 10^{19} \text{ m}^{-3}$ . That of the edge PMT system can give a good estimation even for the extremely low  $n_e$  ( $\sim 1 \times 10^{18} \text{ m}^{-3}$ ) and low  $T_e$  ( $\sim 10 \text{ eV}$ ) condition. Since 1991 the edge PMT has been operational, PDA since 1992 and the core PMT since 1993. The two independent groups of the ADC and memory CAMAC have been used for the acquisition of plasma background (BG) light and Thomson scattering (SG) light separately in the PMT signal flow. Shorter time delay in acquiring SG and BG data can reduce more the fluctuation of signal level caused by the edge localized mode (ELM) activity in the subtraction procedure of BG data from SG data. The precise edge profiles of  $T_e$  and  $n_e$  have been possible to be obtained even with giant ELM activity, when the time delay of the SG and BG timings is shortened to less than 200 ns.

## 5. Data Acquisition System and Data Processing System

The Thomson scattering spectrum is reconstructed with the acquired data from the corresponding CAMAC memories and also with the corresponding calibration data of relative sensitivity of spectral channels, spectral slit functions, relative detector and/or amplifier gains, Rayleigh scattered light intensities, laser energy and so on. The estimation of  $T_e$  and  $n_e$  together with their error bars is made through a non-linear least squares fit of fully relativistic Thomson scattering spectrum to measured one. In this procedure a detector shot noise, a plasma background light level and a circuit noise are taken into consideration. As the fully relativistic Thomson scattering spectrum, an analytic formula is used which is applicable to a wide range of plasmas with extremely high accuracy of less than 0.1% at 100 keV.<sup>10)</sup>

## 6. Measurement Examples and Related Discussions

The multilaser operation has been utilized in the transient phenomena measurements of L- to H-mode transition experiments, negative magnetic shear experiments, the pellet injection experiments and so on. Figure 8 shows the  $T_e$  and  $n_e$  profiles just before and 10 ms after the pellet injection to the OH plasma. The particle fueling in the center region of plasma volume by the pellet injection is clearly observed from the change of  $n_e$  profiles before and after the pellet injection.

The precise profiles of  $T_e$  and  $n_e$ , which were obtained through the plasma edge measurement system including the collection and fiber optics with the high spatial resolution (8 mm), the

spectrometer with the high spectral resolution and the highly sensitive PMTs, have enabled the research on the local transport in the plasma edge region. Figure 10 shows the edge transport barrier with spatially steep gradients of  $T_e$  formed at L- to H-mode transition. The measured width of the barrier was 2.4~5.6 cm.<sup>11)</sup>

The profile data from the core and edge measurement systems have been of use to investigating the global confinement of the OH and/or NB heated plasmas and the NB current driven plasmas, and also studying the heating and current driving characteristics of ICRF and LHRF experiments. In the negative shear experiments, started from 1995, the PDA detector system has shown a good performance for higher  $T_e$  plasma measurements. Figure 9 is a typical profile shape of  $T_e$  and  $n_e$  in NB and ICRF heated negative shear plasma, indicating that the formation of the internal transport barrier is recognized even for electrons from the existence of the steep gradient in both  $T_e$  and  $n_e$  measurements. The curve of  $T_e$  profile in Fig. 9 is drawn on the basis of the reliable PDA data. The clear and steep gradient in both  $T_e$  and  $n_e$  profiles is a distinctive feature of the JT-60U negative shear experiment.<sup>12)</sup>

As to higher  $T_e$  plasma measurements, there has been another different problem that the underestimation of  $T_e$  and  $n_e$  is enhanced more through the distortion of Thomson scattering spectrum caused by the deposited film on viewing window surface during normal plasma discharges. For solving this problem, an *in situ* window transmission monitoring by inferring it precisely from a known attenuation of the deposited film has been developed in the JT-60U Thomson scattering system. Also the practicability of an *in situ* window cleaning based on a laser blow-off technique has been investigated extensively. Although the existence of the chromatic upper limit was found in the recovered transmission after the blow-off cleaning, it has been demonstrated that the residual thin film gives the systematic errors only of less than 3% to an apparent measurement of  $n_e$  and  $T_e$  at 10 keV or less. The attenuation itself is unchanged before and after the laser blow-off cleaning. So a complementary use of both methods can provide the Thomson scattering measurement of high  $T_e$  plasmas with durable reliability and sufficient precision.<sup>13)</sup>

## 7. Conclusion

The JT-60U Thomson scattering system with new design concepts has been operated since 1991, and shown fully its high performance. The measured data of  $T_e$  have been in good agreement with ECE data. And the line integrated  $n_e$  data along the beam path line in the plasma have been also consistent with the FIR data measured along a similar path line. The following good results have been prominently achieved along the research direction of the JT-60U program that aims at the study of improving the energy confinement with high

spectrometer with the high spectral resolution and the highly sensitive PMTs, have enabled the research on the local transport in the plasma edge region. Figure 10 shows the edge transport barrier with spatially steep gradients of  $T_e$  formed at L- to H-mode transition. The measured width of the barrier was 2.4~5.6 cm.<sup>11)</sup>

The profile data from the core and edge measurement systems have been of use to investigating the global confinement of the OH and/or NB heated plasmas and the NB current driven plasmas, and also studying the heating and current driving characteristics of ICRF and LHRF experiments. In the negative shear experiments, started from 1995, the PDA detector system has shown a good performance for higher  $T_e$  plasma measurements. Figure 9 is a typical profile shape of  $T_e$  and  $n_e$  in NB and ICRF heated negative shear plasma, indicating that the formation of the internal transport barrier is recognized even for electrons from the existence of the steep gradient in both  $T_e$  and  $n_e$  measurements. The curve of  $T_e$  profile in Fig. 9 is drawn on the basis of the reliable PDA data. The clear and steep gradient in both  $T_e$  and  $n_e$  profiles is a distinctive feature of the JT-60U negative shear experiment.<sup>12)</sup>

As to higher  $T_e$  plasma measurements, there has been another different problem that the underestimation of  $T_e$  and  $n_e$  is enhanced more through the distortion of Thomson scattering spectrum caused by the deposited film on viewing window surface during normal plasma discharges. For solving this problem, an *in situ* window transmission monitoring by inferring it precisely from a known attenuation of the deposited film has been developed in the JT-60U Thomson scattering system. Also the practicability of an *in situ* window cleaning based on a laser blow-off technique has been investigated extensively. Although the existence of the chromatic upper limit was found in the recovered transmission after the blow-off cleaning, it has been demonstrated that the residual thin film gives the systematic errors only of less than 3% to an apparent measurement of  $n_e$  and  $T_e$  at 10 keV or less. The attenuation itself is unchanged before and after the laser blow-off cleaning. So a complementary use of both methods can provide the Thomson scattering measurement of high  $T_e$  plasmas with durable reliability and sufficient precision.<sup>13)</sup>

## 7. Conclusion

The JT-60U Thomson scattering system with new design concepts has been operated since 1991, and shown fully its high performance. The measured data of  $T_e$  have been in good agreement with ECE data. And the line integrated  $n_e$  data along the beam path line in the plasma have been also consistent with the FIR data measured along a similar path line. The following good results have been prominently achieved along the research direction of the JT-60U program that aims at the study of improving the energy confinement with high

plasma performance, the study of the steady-state capability and the provision of high quality data needed for advancing the ITER physics R&D and developing the conceptual design of a commercially attractive tokamak reactor with steady-state operation.

(1) The multi-ruby-laser system

The first demonstration using a beam combine method has been done in the JT-60U Thomson scattering system. The minimum time delay of 2 ms between the two ruby lasers have been utilized effectively for the transient phenomena measurements.

(2) The highest spatial resolution of 8 mm

The precise measurement of the transport barrier formed in the plasma edge region can be made with the highest spatial resolution in all the Thomson scattering diagnostics operated in the tokamak devices. The dual data acquisition system for Thomson scattering light and plasma light separately with the time delay of less than 200 ns can also provide the precise  $T_e$  and  $n_e$  profile measurements in the plasma edge region, suppressing the effect of the ELM activities.

(3) The most multipoint with 60 spatial channels

An accurate appraisal of JT-60U plasma performance can be made through  $T_e$  and  $n_e$  profile measurements with 60 spatial channels. The number of 60 measurable points is the most spatial channels in all the Thomson scattering diagnostics operated in the tokamak devices. This multipoint measurement can be attained mainly through the two collection optics (the improved double Gaussian lens and the newly developed Cassegrain mirrors) and the PDA/PMT detector systems.

(4) The reliable measurement of high  $T_e$  plasmas by the high repetition PDA detector system

The newly developed PDA detector system with the division of the wide spectral range into 12 pixels can provide the reliable measurement of high  $T_e$  plasmas especially produced in discharges with the negative magnetic shear. The high repetition capability of less than 1 ms also enables the PDA detector system to measure the transient phenomena together with the burst mode operation of the multi-ruby-laser system. As to the window coating problem which distorts the Thomson scattering spectrum particularly in higher  $T_e$  plasmas, the two solutions have been developed: the *in situ* window transmission inferring method and the laser blow-off window cleaning method. The former method has successfully been working in the data processing logic for correcting the underestimation of apparently measured  $T_e$  and  $n_e$  values.

(5) The exact  $n_e$  measurement by the direct and quantitative alignment method

The newly developed direct and quantitative alignment method for its monitoring and restoration can give the system the compatibility of a stable maintenance of alignment

with an improvement of the  $S/N$  ratio of Thomson scattering to plasma light. Together with high spatial resolution, this alignment method can ensure the accurate  $n_e$  measurement in the plasma edge region.

### **Acknowledgments**

The authors would like to appreciate Dr. T. Matoba and Dr. D. Johnson (Plasma Physics Laboratory of Princeton University) for useful discussions and suggestions, and Dr. M. Mori, Dr. A. Funahashi and Dr. H. Kishimoto for their continuous support and encouragement. The authors gratefully acknowledge T. Sakuma, Y. Onose, Y. Suzuki and D. Kazama for their technical assistance in operation and calibration of the JT-60U Thomson scattering system.



with an improvement of the  $S/N$  ratio of Thomson scattering to plasma light. Together with high spatial resolution, this alignment method can ensure the accurate  $n_e$  measurement in the plasma edge region.

### **Acknowledgments**

The authors would like to appreciate Dr. T. Matoba and Dr. D. Johnson (Plasma Physics Laboratory of Princeton University) for useful discussions and suggestions, and Dr. M. Mori, Dr. A. Funahashi and Dr. H. Kishimoto for their continuous support and encouragement. The authors gratefully acknowledge T. Sakuma, Y. Onose, Y. Suzuki and D. Kazama for their technical assistance in operation and calibration of the JT-60U Thomson scattering system.

## References

- <sup>1</sup>N. Bretz, D. Dimock, V. Foote, D. Johnson, D. Long and E. Tolnas, *Appl. Opt.* **17**, 192 (1978).
- <sup>2</sup>D. Johnson, N. Bretz, D. Dimock, B. Grek, D. Long, R. Palladino and E. Tolnas, *Rev. Sci. Instrum.* **57**, 1856 (1986).
- <sup>3</sup>H. Rohr, K.-H. Steuer, H. Murmann and D. Meisel, "Periodic Multichannel Thomson Scattering in ASDEX," IPP Report III/121 B, 1987.
- <sup>4</sup>H. Saltzmann, J. Bundgaard, A. Gadd, C. Gowers, K. H. Hansen, K. Hirsch, P. Nielsen, K. Reed, C. Schodter and K. Weisberg, *Rev. Sci. Instrum.* **59**, 1451 (1988).
- <sup>5</sup>C. L. Hsieh, R. Chase, J. C. DeBoo, R. G. Evanko, P. Gohil, R. T. Snider and R. E. Stockdale, *Rev. Sci. Instrum.* **59**, 1467 (1988).
- <sup>6</sup>H. Yokomizo, H. Yoshida, M. Sato, A. Nagashima, Y. Mabuchi and Y. Miura, *Kakuyugo Kenkyu* **59**, Suppl. 72 (1988), in Japanese.
- <sup>7</sup>T. N. Carlstrom, G. L. Campbell, J. C. DeBoo, R. G. Evanko, J. Evans, C. M. Greenfield, J. S. Haskovec, C. L. Hsieh, E. McKee, R. T. Snider, R. Stockdale, P. K. Trost and M. P. Thomas, *Rev. Sci. Instrum.* **63**, 4901 (1992).
- <sup>8</sup>H. Yoshida, O. Naito, O. Yamashita, S. Kitamura, A. Nagashima and T. Matoba, *Rev. Sci. Instrum.* **66**, 143 (1995).
- <sup>9</sup>H. Yoshida, O. Naito, O. Yamashita, S. Kitamura, T. Hatae and A. Nagashima, to be published in *Rev. Sci. Instrum.* (1997).
- <sup>10</sup>O. Naito, H. Yoshida and T. Matoba, *Phys. Fluids B* **5**, 4256 (1993).
- <sup>11</sup>M. Kikuchi, H. Shirai, T. Takizuka, Y. Kamada, Y. Koide, H. Yoshida, O. Naito, T. Fujita, T. Nishitani, N. Isei, M. Sato, T. Fukuda, S. Tsuji, H. Kubo, T. Sugie, N. Asakura, N. Hosogane, H. Nakamura, M. Shimada, R. Yoshino, H. Ninomiya, M. Kuriyama, M. Yagi, K. Tani, A. A. E. Van Blockland, T. S. Taylor, G. L. Jackson, D. J. Campbell, D. Stork, A. Tanga and JT-60 Team, *Nuclear Fusion Supplement (Proc. 14th Int. Conf. on Plasma Physics and Controlled Nuclear Fusion Research, Wurzburg, 1992)*, IAEA, Vienna, Vol. 1, 189~203 (1993).
- <sup>12</sup>H. Kimura and the JT-60 Team, *Phys. Plasmas*, **3**, 1943 (1996).
- <sup>13</sup>H. Yoshida, O. Naito, T. Hatae and A. Nagashima, to be published in *Rev. Sci. Instrum.* (1997).

Table I. Laser system, beam combiner and beam input optics

	Ruby Laser 1 (PDS4, Lumonics)	Ruby Laser 2 (PDS2s, Lumonics)
<b>Ruby Lasers</b>		
energy ( J)	2.5, 5, 10, 20	10
pulse interval ( sec)	1, 2, 4, single	4
pulse width (nsec)	30	30
divergence ( $\mu$ rad)	less than 300	less than 300
polarization	P	S
diameter ( mm)	26	22
<b>Beam Combiner</b>		
polarizer plate	transmission	reflection
Faraday rotation angle	90° (PDS4only)	
total energy loss	less than 5%	less than 2%
minimum time interval of 2 lasers	2 msec	
<b>Faraday rod</b>		
dimension (mm)	45 $\phi$ x 40length	
Verdet const. (min./Oe/cm)	-0.242 at 632.8 nm	
<b>solenoid</b>		
dimension (mm)	64 $\phi$ x 197length	
coil current (A)	~800	
number of turns	150	
<b>Beam Optics</b>		
number of bending mirrors	8 (a single beam path line)	
focusing lens	f/9.75m (beam diameter in vessel : 3~7 mm)	
beam dump	colored filter glass	
energy monitor	integrating sphere with ND filter and Fresnel lens after beam dump optical fiber(~300m), PIN diode, gated ADC/CAMAC	

Table II. Parameters of collection optics, fiber optics and alignment system

	Plasma Edge Measurement	Plasma Core Measurement
Collection Optics	Gaussian type lens	Cassegrain type reflection mirror
effective field of view	18°	46°
span of measurement (m)	0.7	1.4
F number	F/2.1	
focal length (mm)	340	225.57
magnification	-0.22	-0.16
transmission	90%	75%
solid angle (sr)	0.0065	0.0055
window size (mm)	260	260
shutter	yes	yes
Fiber Optics		
core/clad diameter (μm)	180/200, quartz	180/200, quartz
I/O bundle size (mm)	1.73 <sup>h</sup> x1.59 <sup>w</sup> and 0.80 <sup>h</sup> x3.50 <sup>w</sup> 3.50 <sup>h</sup> x1.42 <sup>w</sup> and 1.50 <sup>h</sup> x3.40 <sup>w</sup>	3.50 <sup>h</sup> x1.07 <sup>w</sup> and 1.60 <sup>h</sup> x2.40 <sup>w</sup>
N <sub>A</sub>	~0.3	~0.3
length(m)	104	104
transmission (He-Ne)	45~50%	45~50%
measurement bundles	30	30
alignment bundles	4	4
Alignment System		
for object field of collection fiber optics		
parallel correction (Bt direction)	±6.5 mm (0.001mm step)	±5.5 mm (0.001mm step)
rotation correction on optical axis	±6.5° (0.001° step)	±3.5° (0.001° step)
direct & quantitative alignment monitor and recovery	yes	yes
for beam optics	remote correction with monitoring beam burn pattern through CCD cameras and adjusting computer-controlled mirror gimbal	

Table III. Parameters of spectrometers and coupling optics.

	Plasma Edge Measurement	Plasma Core Measurement
Spectrometers	Littrow x 1 (PMT system)	Littrow x 2 (PMT & PDA systems)
F number	2.9	2.9
focal length (mm)	275	275
grating (1/mm)	1200	600
grating size (mm)	97x100	102x102
output image size (mm)	60.0 <sup>h</sup> x51.3 <sup>w</sup>	60.0 <sup>h</sup> x51.3 <sup>w</sup>
spectral range (nm)	550~688	403~683
Fiber Bundles from Spectrometer to PMTs		
core	glass	glass
clad diameter ( $\mu\text{m}$ )	50	50
$N_A$	0.57	0.57
length (m)	~2.3	~2.5
transmission	50~60%	50~60%
number of bundles	130 ch [spatially 30 and spectrally (4~5) ]	60 ch [spatially 10 and spectrally 6 ]
Wavelength Cut Glass for Plasma Core Measurement by PDA System		
width in dispersion direction		4.0 mm for Ruby (694.3 nm) 4.0 mm for $H_{\alpha}/D_{\alpha}$ emission 3.8 mm for $H_{\beta}/D_{\beta}$ emission
Coupling Lens for Plasma Core Measurement by PDA System		
field lens		achromat lens (made to order)
coupling lens		Canon EF50mm/F1.0L

Table IV. Parameters of PDA/PMT detector systems

	PMT System for Plasma Edge & Core Measurement	PDA System for Plasma Core Measurement
Detectors	photomultiplier tube (PMT: R943-03)	proximity focused type image intensifier + 2 dimensional photodiode array (PDA)
photocathode size (mm)	10 x 10 (GaAs)	25 <sup>φ</sup> (S-20)
photodiode size (mm)		17.42 x 13.84
quantum efficiency		
photocathode	0.13 (400~700 nm)	0.16 at 400 nm, 0.03 at 694.3 nm
photodiode		0.93 at 400 nm (peak wavelength of P-47)
phosphor decay time (nsec)		~0.2 (P-47)
ADC gate width (μsec)	0.125	0.125
A/D conversion bits	( 11 in LeCroy 4301B)	12
A/D conversion time (μsec)	(~10 in LeCroy 4301B)	max. 3
data transfer time (μsec)		480 (signal 240 ch + background 240 ch)
number of elements		
for edge measurement	130 PMTs = spatially 30 x spectrally (4~5)	
for core measurement	60 PMTs = spatially 10 x spectrally 6	240 ch /unit = spatially 20 x spectrally 12
dynamic range	more than 10 <sup>5</sup>	~10 <sup>3</sup>

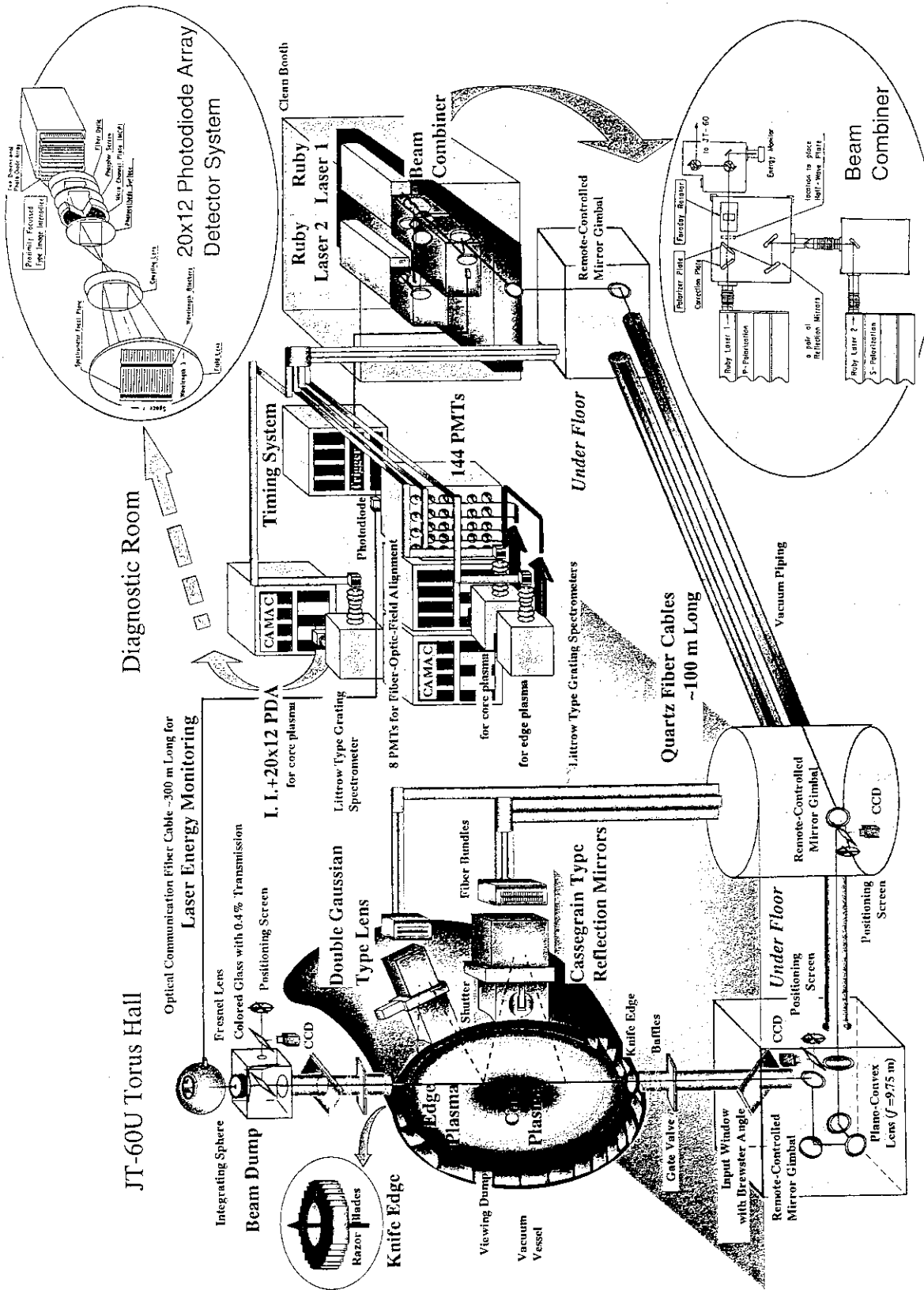


Figure 1

Schematic layout of the JT-60U Thomson scattering system. The distance from the two ruby lasers to the plasma is about 70 m. Newly developed components of 20x12 photodiode array detector and beam combiner are shown in the expanded illustrations

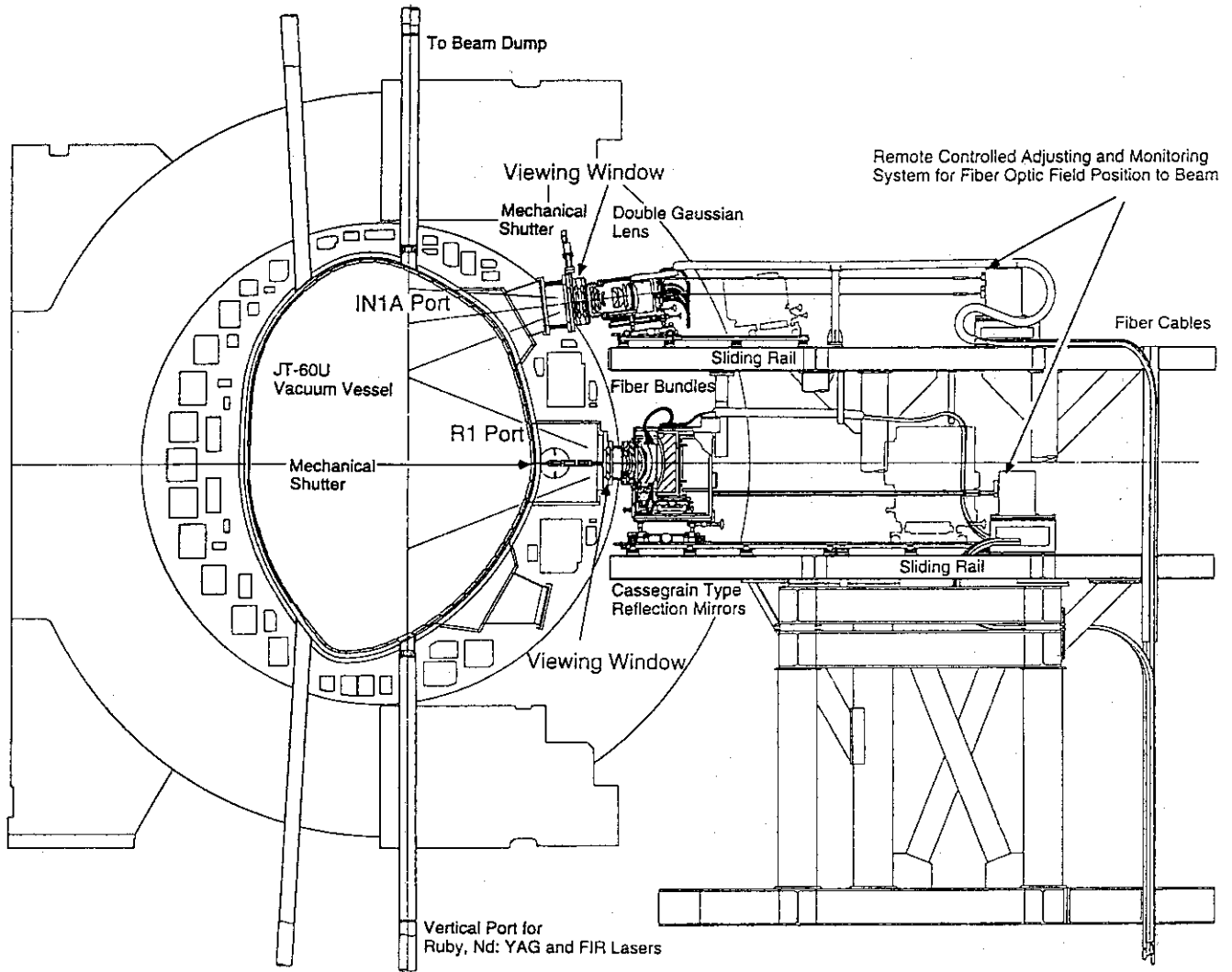


Figure 2

Layout of the two collection optics which view the different laser scattering volumes along a single beam path line from the corresponding viewing windows at *IN1A* and *R1* ports



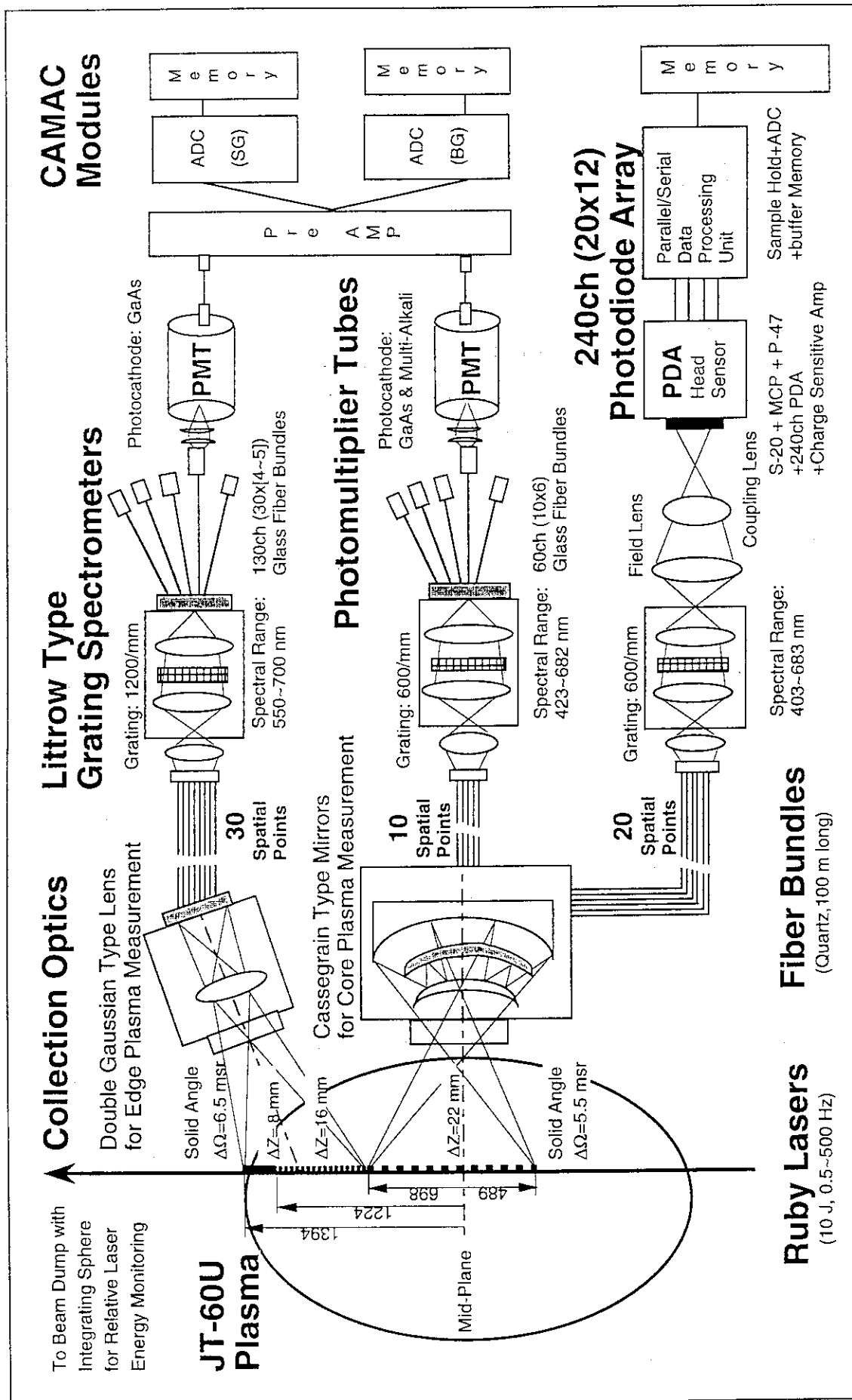


Figure 3

Schematic illustration of ruby lasers, collection and fiber optics, detector systems and data acquisition systems in the JT-60U Thomson scattering diagnostic

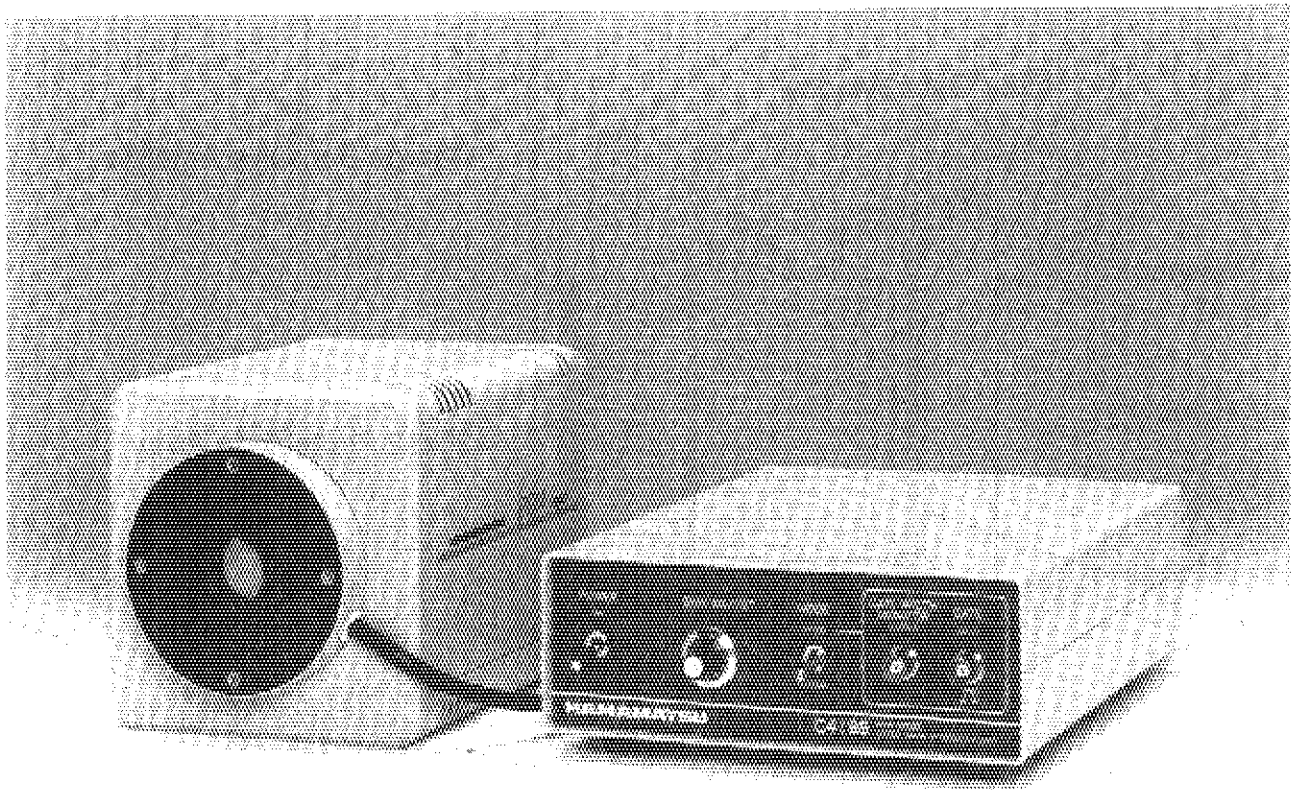


Figure 4  
Photograph of the newly developed two-dimensional detector for higher  $T_e$  plasma measurement

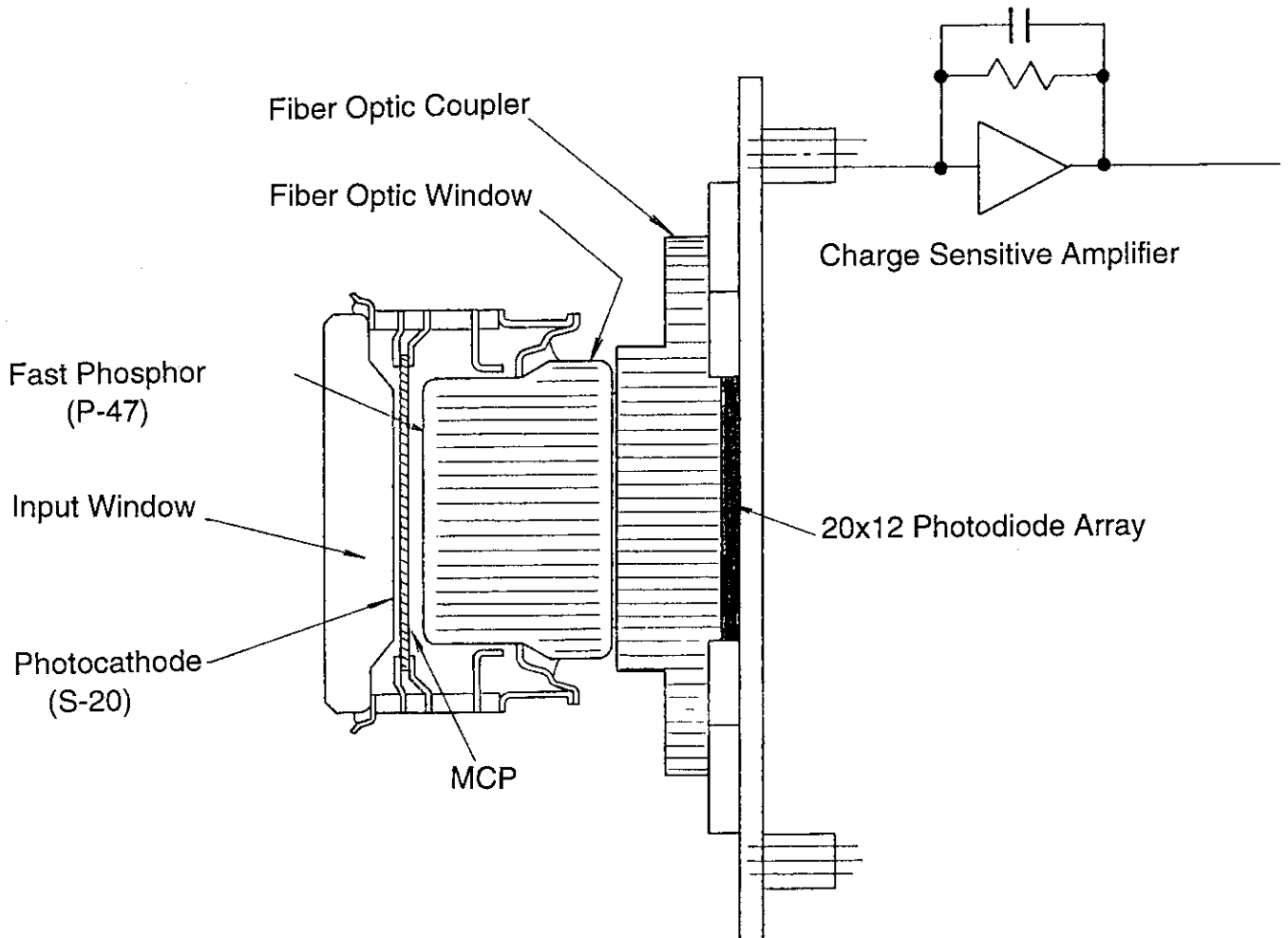


Figure 5  
Schematic structure of the newly developed two-dimensional detector

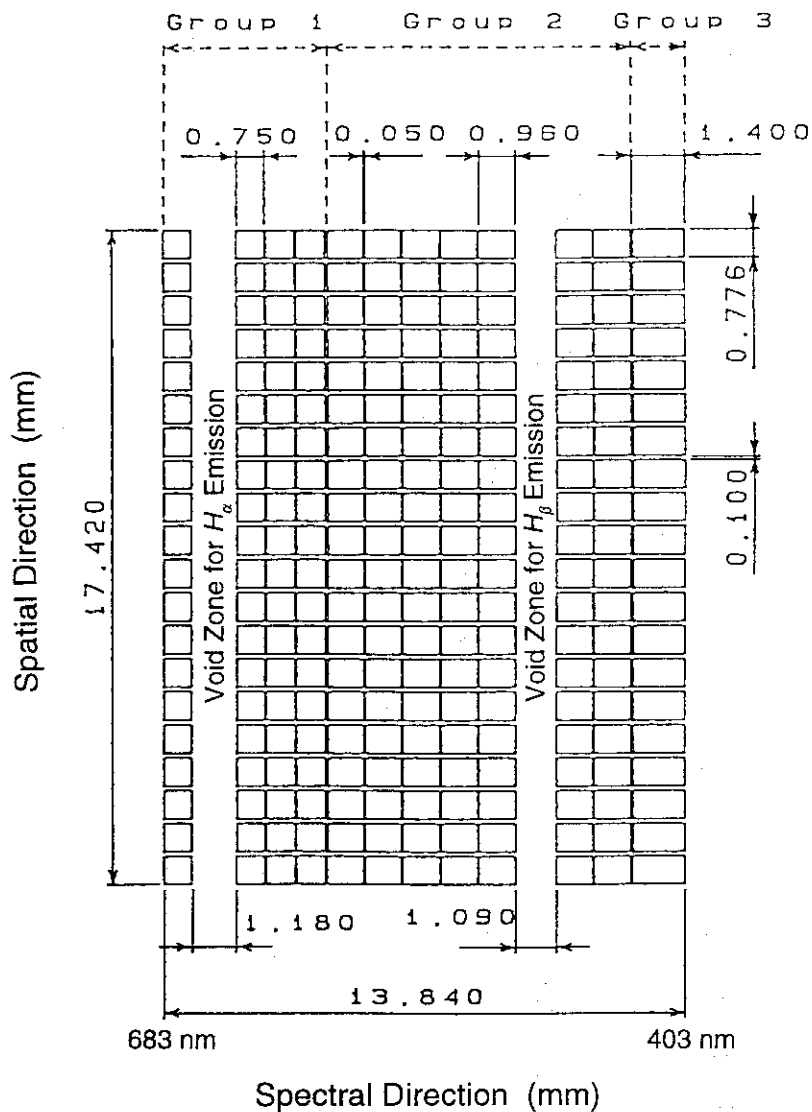


Figure 6

Spatial and spectral division of photodiode array (PDA) elements. Wide spectral range of 403~683 nm with 12 spectral division for each spatial point enables PDA detector to measure higher electron temperature up to 20 keV

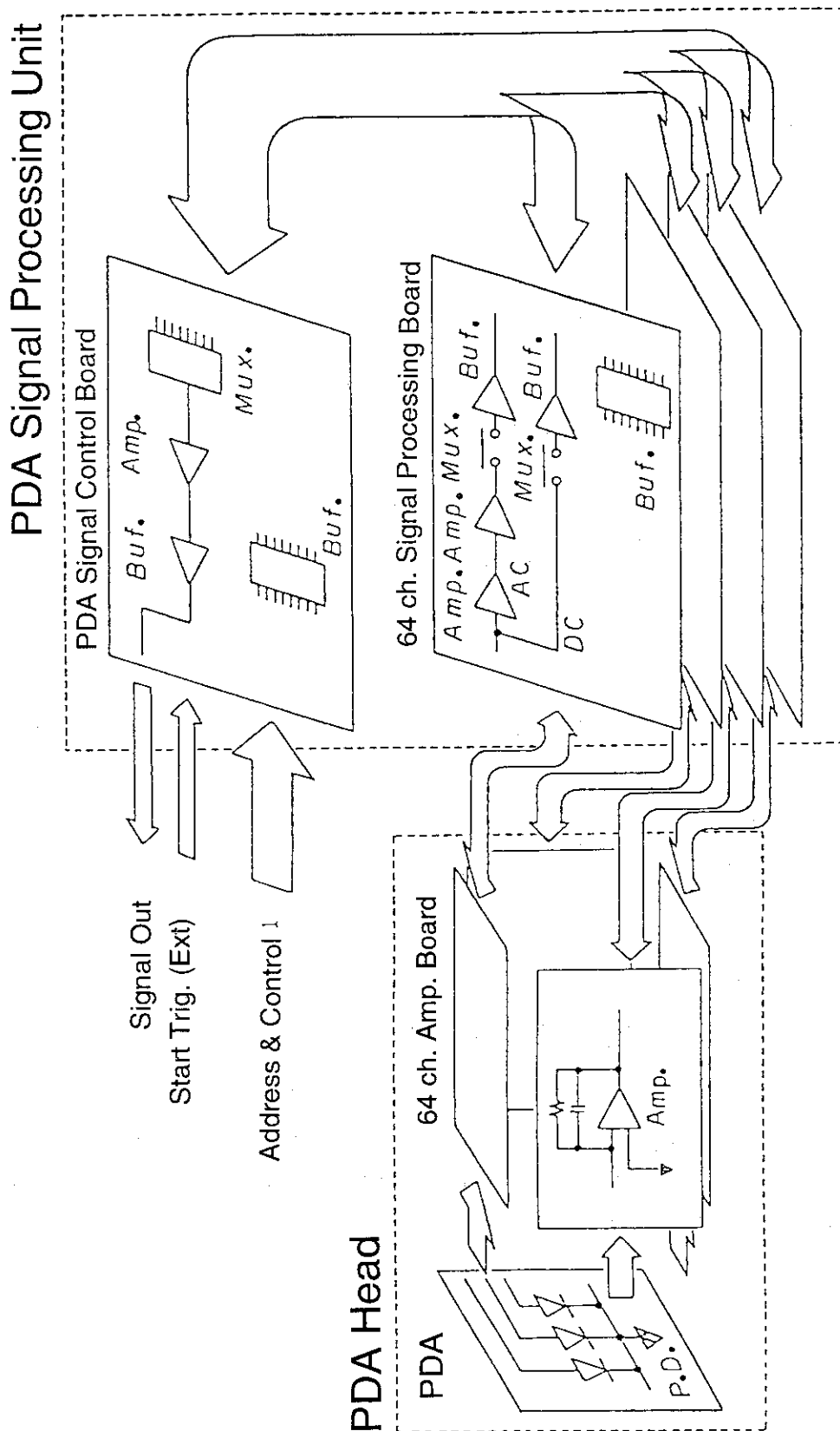


Figure 7  
Schematic illustration of PDA data flow with parallel processing for higher repetition measurement of less than 1 ms

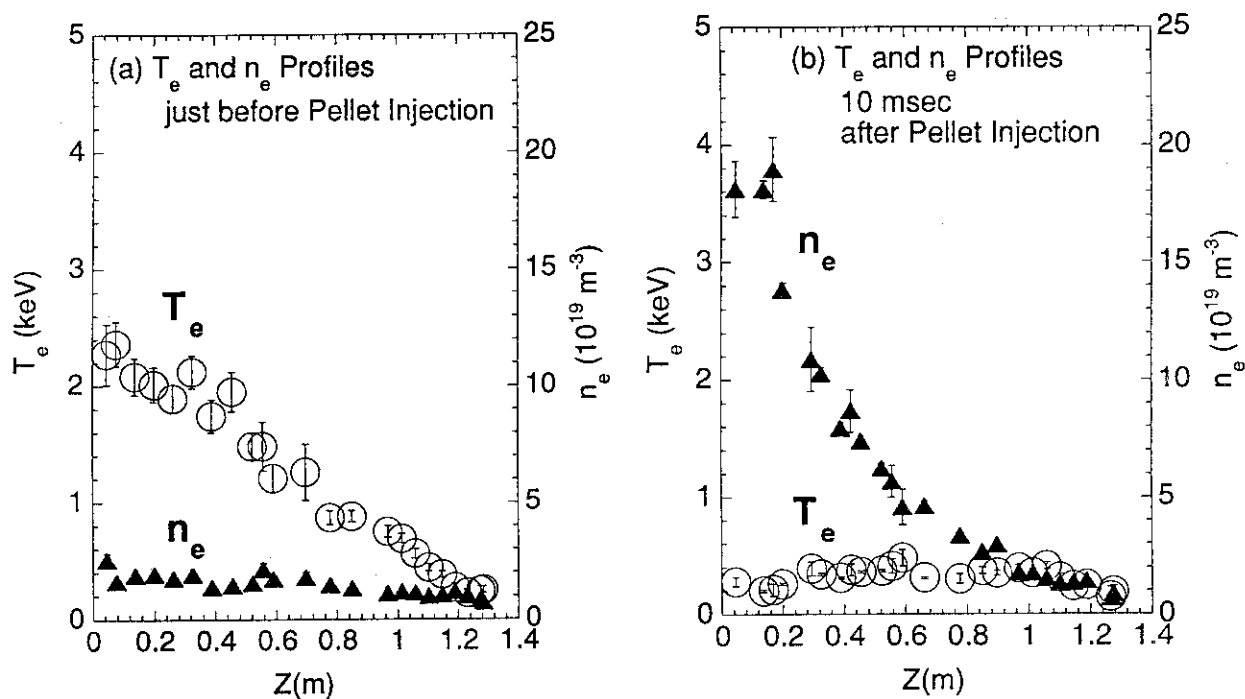


Figure 8

Measurement example of the change of  $T_e$  and  $n_e$  profiles just before and 10 ms after the pellet injection to the OH plasma, which were measured through the effective use of multilaser operation

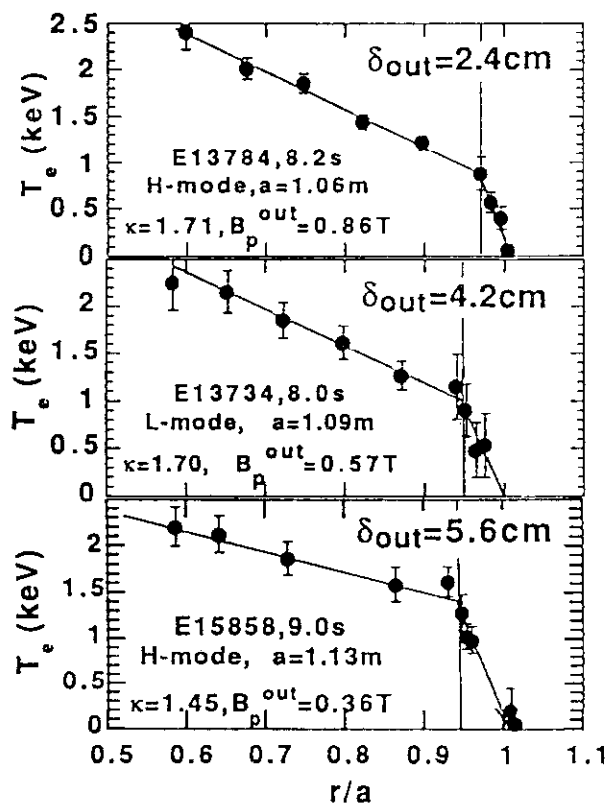


Figure 9

Measurement example of edge transport barrier formed at L- to H-mode transition

# Negative Shear Experiment (NB + IC Heating)

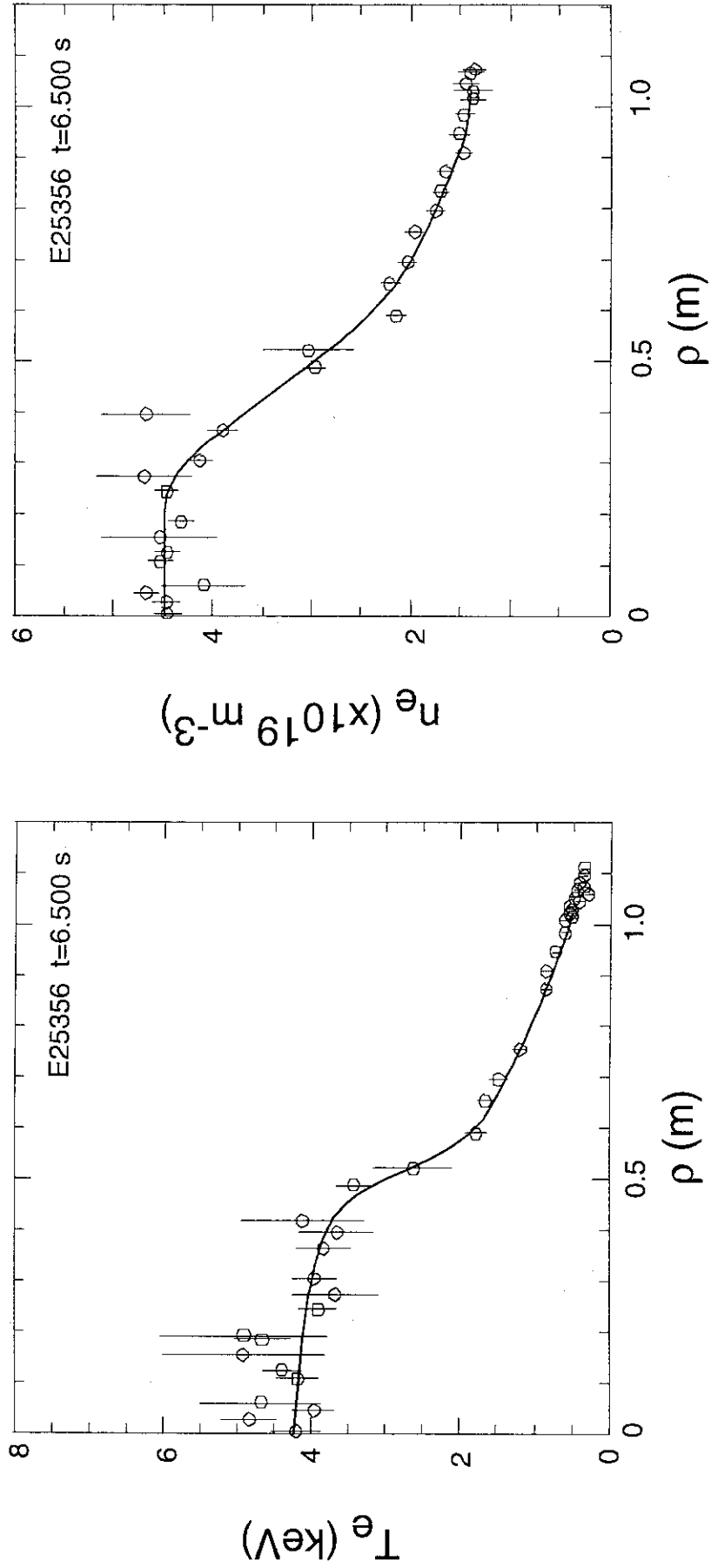


Figure 10

Measurement example of profile shapes of  $T_e$  and  $n_e$  in NB and ICRF heated negative shear plasma. The internal transport barrier with steep gradient of  $T_e$  and  $n_e$  profiles is a distinctive feature of the JT-60U negative shear experiment